liquid drop has been made with precision comparable to the static investigations of Cohen and Swiatecki.[5] Both Kelson's and Nix's simplified dynamical treatments[9,10] provide static saddle-point properties which agree best with Cohen and Swiatecki's[5] for elements less massive than radium (fissionability parameter $\simeq 0.70$). It is hoped that the present investigations will provide a few-parameter basis for dynamical calculations of adequate precision, even for $x$ values approaching 1.00. Studies directed towards this goal are presently under way.

**ACKNOWLEDGMENTS**

This investigation was suggested by Dr. James J. Griffin of the University of California, Los Alamos Scientific Laboratory, as a part of the research of a Ph.D. thesis problem for the Graduate School of Vanderbilt University. I am deeply indebted to Dr. Griffin for his advice in many enlightening discussions. The continued interest and encouragement of Dr. William T. Pinkston of Vanderbilt University is also appreciated.

PHYSICAL REVIEW VOLUME 139, NUMBER 5B 6 SEPTEMBER 1965

# Inelastic Scattering and Neutron Pickup for $^{12}C$ and $^{16}O$ Projectiles on $^{208}Pb$*†

K. H. WANG‡ AND J. A. MCINTYRE§
*Physics Department, Yale University, New Haven, Connecticut*
(Received 1 February 1965; revised manuscript received 6 May 1965)

$^{208}Pb$ nuclei have been bombarded with $^{12}C$ and $^{16}O$ projectiles under conditions where a semiclassical description of the process should be valid. In the bombardment of $^{208}Pb$ with 126.5-MeV $^{12}C$ ($\eta = ZZ'e^2/\hbar v = 24.5$), two inelastic-scattering peaks are observed corresponding to $Q = -2.7 \pm 0.3$ MeV and $-4.5 \pm 0.3$ MeV. The angular distributions of the inelastically scattered $^{12}C$ show a monotonic increase with decreasing angle until a maximum is reached at about $\theta_{c.m.} = 35°$. This angle corresponds to grazing collisions, assuming that particles follow Rutherford trajectories. The $Q = -2.7$-MeV peak is identified as the excitation of the 2.6-MeV state in $^{208}Pb$. The $Q = -4.5$-MeV peak could be the excitation of the 4.4-MeV state in $^{12}C$ or the 4.3-MeV state in $^{208}Pb$. The inelastic scattering cross section for the excitation of the 2.6-MeV $^{208}Pb$ state by $^{16}O$ projectiles having approximately the same velocity (166.4 MeV) is a factor of 2 smaller than when $^{12}C$ is used as a projectile; this result is somewhat surprising since the semiclassical conditions are similar and the elastic-scattering cross sections differ only by 20%. The cross section for the 4.5-MeV excitation is not observed and is smaller by more than a factor of 4. Therefore, in the $^{12}C + ^{208}Pb$ case, the major contribution to the 4.5-MeV excitation very likely originates from the excitation of the 4.4-MeV state in $^{12}C$. The reactions $^{208}Pb(^{16}O, ^{17}O)^{207}Pb$ and $^{208}Pb(^{12}C, ^{13}C)^{207}Pb$ were also observed in these experiments. Both angular distributions have a maximum differential cross section of 100 mb/sr, which is considerably larger than those ordinarily observed in neutron-transfer reactions. The excitation energies are consistent in both reactions with neutrons being picked up by the projectiles into $d_{5/2}$ states.

## I. INTRODUCTION AND SUMMARY

IN recent years, it has been found that in inelastic scattering, the collective levels are more strongly excited than others, regardless of the projectiles used. The preferential excitation of collective levels by alpha particles has been pointed out by Blair.[1] Cohen[2] has noted the similarity between the inelastic scattering of protons and deuterons and has emphasized the collective nature of the process. High-energy electron scattering[3] has been shown to strongly excite levels known to be collective. Heavy-ion ($^{12}C$) inelastic scattering has also been shown [4,5] to be very similar to the alpha-particle scattering. This enhancement can be understood in terms of the similarity between the matrix elements of inelastic scattering and electric transitions, as pointed out by Pinkston and Satchler.[6] Therefore regardless of the projectiles used, the inelastic-scattering process has proved to be a good method for investigating collective states.

In the heavy-ion studies of inelastic scattering, the

* Supported by the U. S. Atomic Energy Commission.
† Part of a dissertation presented by K. H. Wang in partial fulfillment of the requirements for the Ph.D. degree of Yale University.
‡ Present address: Harvard Cyclotron Laboratory, Cambridge, Massachusetts.
§ Present address: Physics Department, Texas A & M University, College Station, Texas.
[1] J. S. Blair, Phys. Rev. **115**, 928 (1959).
[2] B. L. Cohen, Phys. Rev. **116**, 426 (1959); B. L. Cohen and R. E. Price, *ibid.* **123**, 283 (1961).
[3] H. Crannel, R. Helm, H. Kendall, J. Oeser, and M. Yearian, Phys. Rev. **123**, 923 (1961). H. W. Kendall and J. Oeser, *ibid.* **130**, 245 (1963).
[4] S. D. Baker, K. H. Wang, and J. A. McIntyre, *Proceedings of the International Conference on Nuclear Structure, Kingston, 1960* (University of Toronto Press, Toronto, 1960), p. 926; K. H. Wang, S. D. Baker, and J. A. McIntyre, Phys. Rev. **127**, 187 (1962).
[5] D. J. Williams and F. E. Steigert, Nucl. Phys. **30**, 373 (1962).
[6] W. T. Pinkston and G. R. Satchler, Nucl. Phys. **27**, 270 (1960).

nuclear-deformation parameter $\beta$ has been evaluated using the Blair diffraction model[1] as well as the more accurate distorted-wave Born theory.[7] In addition, the properties of the excited levels have been investigated in some detail.[8]

The elastic-scattering process may be described semiclassically if the parameter $\eta$ is large.[9] This has been demonstrated by the success of the sharp cutoff model[10] of Blair. The classical nature of the collision process often simplifies the theoretical calculation and also gives a physical picture which can aid in understanding the scattering. All of the inelastic scattering work discussed so far has been performed under conditions where the beam of ions can be considered to a good first approximation as a plane wave. In particular, the Coulomb interaction parameter[9] $\eta$ has been of the order of unity. When $\eta$ is large, the inelastic scattering could be described, presumably, in a semiclassical manner in contrast to the diffraction description used for small values of $\eta$. It would be of interest to investigate the effect of this parameter on inelastic scattering, and in particular, to determine if it might be possible to make use of the physical intuition associated with classical problems.

In the experiments reported in this paper, $^{208}$Pb is bombarded with 126.5-MeV $^{12}$C($\eta=24.5$). Two inelastic peaks are observed in the energy spectrum corresponding to excitation energies of 2.7 and 4.5 MeV. These peaks are associated, respectively, with the excitation of the 2.6-MeV level in $^{208}$Pb and with either the excitation of the 4.3-MeV level in $^{208}$Pb or of the 4.4-MeV level in $^{12}$C. The angular distributions of both peaks show a monotonic increase with decreasing angle, leveling off at about $\theta_{\text{c.m.}}=35°$ (see Figs. 4 and 5). The angular distribution of the 4.5-MeV peak shows a further decrease at smaller angles. The maximum of the cross section occurs at an angle corresponding to grazing collisions, assuming that particles follow Rutherford trajectories. When 166.4 MeV $^{16}$O (same velocity as $^{12}$C ions) are scattered from $^{208}$Pb, the cross section of the inelastic scattering leading to 2.7-MeV excitation is found to be smaller than that for $^{12}$C on $^{208}$Pb by approximately a factor of 2. This difference is surprising since the scattering conditions for the $^{12}$C and the $^{16}$O experiments are semiclassically almost identical, this fact being reflected in the elastic scattering cross sections which differ by only 20%. Nevertheless, the $^{12}$C projectile cross sections for exciting the 2.6-MeV level in $^{208}$Pb is twice that for the $^{16}$O projectile. Also, there is no 4.5-MeV excitation produced in the $^{16}$O experiment (a reduction of at least a factor of 4). The absence of the 4.5-MeV excitation with the $^{16}$O as projectile indicates that the 4.5-MeV excitation with the $^{12}$C projectile corresponds, most likely, to excitation of the $^{12}$C itself.

An additional peak also appears in the energy spectra of both $^{12}$C and $^{16}$O. These peaks have been identified as $^{13}$C and $^{17}$O peaks, respectively, corresponding to neutron pickup reactions. Both pickup angular distributions have a maximum at about the same angle as the inelastic scattering and the magnitude is about 100 mb/sr. This is approximately two to four times larger than the single-neutron stripping heretofore measured at the same ion velocity with the exception[11] of $^{19}$F. From the energy considerations, the reaction of $^{208}$Pb($^{16}$O,$^{17}$O)$^{207}$Pb corresponds to the neutron being picked up in the ground $d_{5/2}$ state of $^{17}$O. While the level assignment is not unique in the $^{208}$Pb($^{12}$C,$^{13}$C)$^{207}$Pb reaction, the neutron transfer is consistent with a pickup in the lowest $d_{5/2}$ level in $^{13}$C also. The reason for this preferential pickup is not known. However, similar results have been found in $(\alpha,d)$ reactions by Harvey, Cerny, Pehl, and Rivet.[12]

## II. EXPERIMENTAL APPARATUS

The experimental setup is, in principle, the same as in the $^{12}$C on $^{12}$C experiment.[4] However, a 4-ft-diam scattering chamber has been used in the present work. A schematic diagram is shown in Fig. 1. The detector is placed inside the 4-ft vacuum chamber on a movable arm. The degrading foil which is used for particle identification is placed on another arm which can be rotated independently of the detector arm and the foil can be brought in front of the detector whenever desired. Both arms are attached to shafts concentric with the shaft on which the target holder is mounted.

The beam of particles passes through two slits before entering the chamber. (Only the second, the image slit,

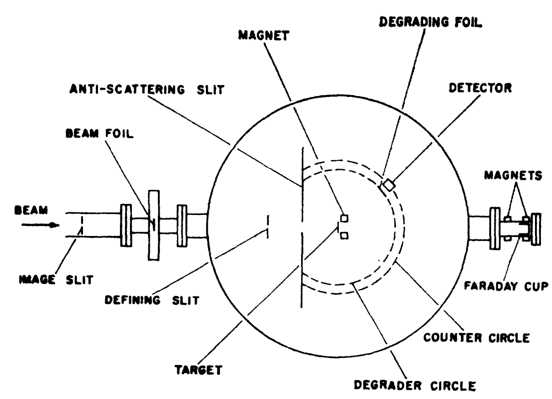


FIG. 1. Schematic diagram of the 4-ft-diam scattering chamber and associated experimental apparatus.

[7] J. C. Hiebert and G. T. Garvey, Phys. Rev. **135**, B346 (1964).
[8] G. T. Garvey, A. M. Smith, and J. C. Hiebert, Phys. Rev. **130**, 2397 (1963).
[9] $\eta$, the Coulomb strength parameter, is defined as $ZZ'e^2/\hbar v$, where $Ze$ and $Z'e$ are the charges of the projectile and target nuclei, $2\pi\hbar$ is Planck's constant, and $v$ is the relative velocity of the projectile and target nuclei.
[10] J. S. Blair, Phys. Rev. **95**, 1218 (1954).
[11] R. Kaufmann and R. Wolfgang, Phys. Rev. **121**, 206 (1961).
[12] B. G. Harvey, J. Cerny, P. H. Pehl, and E. Rivet, Nucl. Phys. **39**, 160 (1962).

is shown in Fig. 1.) The slits are designed to improve the energy resolution of the beam. Good beam energy resolution is necessary since the high-intensity elastic scattering peak can easily mask any nearby inelastic peaks. A beam energy resolution of 0.7% (full width at half-maximum) has been obtained in this manner and was maintained throughout a continuous run of about 90 h.

In heavy-ion reactions, a great number of particles are produced. It is therefore necessary to differentiate the reaction products from inelastically scattered particles. A degrading foil was used in front of the counter for this purpose since particles of different species but of same energy do not lose the same amount of energy in the same absorber. The fact that the energy response of the solid-state detector is independent of the particle species greatly facilitates the absorber method.

The detector was calibrated first without the absorber in front of it by degrading the incident beam with aluminum foils (denoted as beam foil in Fig. 1). With the known incident energy and the thickness of the beam foil, together with Northcliffe's range-energy curve,[13] the energy of the particles striking the target could be obtained. The kinematics of the elastic scattering then determined the energy of the scattered particles that entered the detector and the detector pulse height could be calibrated in terms of the energy of the ion striking the *detector*. This calibration is shown as the $\Delta E$(counter) scale on the top of the energy spectra (Figs. 2 and 6). $\Delta E$ expresses the energy difference between the elastically and nonelastically scattered particles, the latter including reaction products. The absolute energy scale can be obtained from the knowledge of the energy of the elastically scattered particles. $\Delta E$(counter) then means $\Delta E$ measured at the detector as distinguished from $\Delta E$ measured at the target. When there is no absorber between the target and the counter, the two $\Delta E$'s are equal. In this case, although the calibration is done with the beam particles, it is also applicable to particles of other species due to the characteristics of the solid state detector mentioned earlier.

Another energy calibration was then made but with the absorber between the target and the counter. Without having to know the energy loss of the particles in the absorber, the pulse-height response as a function of the energy of the particles leaving the *target* could then be obtained, the energy loss in the absorber being automatically included in the calibration. It should be noted that the latter calibration curve is only applicable to the beam particles. For inelastically scattered beam particles the $\Delta E$ measured at the counter should remain the same, with or without the absorber, while for all other particles the $\Delta E$ at the counter would appear to have shifted.

In order to identify other particles, the thickness of the absorber must be known. With the aid of a set of Northcliffe's range-energy curves,[14] the relative shifts of the peaks in the energy spectra then gave the identity of the particles. The absorbers used in the experiment were made of Mylar of various thicknesses as indicated in the spectra figures. The actual thickness was found by weighing. The equivalent thickness of aluminum was found by using the conversion factor 0.783 mg/cm$^2$ of Mylar to 1 mg/cm$^2$ of aluminum.[15]

The $^{208}$Pb target was made by evaporating the enriched isotope (99.75%) obtained from Oak Ridge National Laboratory, onto a formvar backing. Due to the kinematics, the backing presents no problem in the measurements. The thickness of the target was approximately 500 $\mu$g/cm$^2$.

The scattered particles were detected by an ORTEC[16] surface barrier detector. The beam was stopped in the Farraday cup and the collected charge deposited on a capacitor; the voltage across the capacitor was measured with an electrometer to obtain the relative cross section.

The beam direction was determined by detecting scattered particles on both sides of the beam. Since the particles were not polarized, the cross section was symmetric about the beam. Elastic scattering at a series of small angles (from 8° to 20°) was measured and the relative cross section was found to be inversely proportional to $\sin^4(\theta/2)$, with $\theta$ being the scattering angle in the center-of-mass system. The scattering at small angles was, therefore, predominantly Rutherford scattering. All data were then normalized against the Rutherford scattering to obtain absolute cross section without having to know precisely the target thickness and solid angle subtended. The Rutherford scattering measurement was accurate to better than 3%.

## III. RESULTS

### A. $^{12}$C+$^{208}$Pb

Figure 2 shows three energy spectra obtained from bombarding $^{208}$Pb with $^{12}$C ions and using absorbers of various thicknesses in front of the detector. There are four well-resolved peaks. The first peak at the right results from elastic scattering. In the upper spectrum where no absorber is used, the other three peaks would correspond to inelastic scattering leading to the excited states at 2.7, 4.5, and 6.5 MeV if the particles forming these peaks are predominantly $^{12}$C. When an absorber is placed before the counter, using the calibration curve obtained with the same absorber, the second and third peaks in the two lower figures still give the same excitation energy as shown by the arrows, indicating

[13] L. C. Northcliffe, Phys. Rev. **120**, 1744 (1960).

[14] These curves have not been published. They are computed for aluminum absorber by L. C. Northcliffe from information contained in Table II of Ref. 13.

[15] P. E. Schambra, A. M. Rauth, and L. C. Northcliffe, Phys. Rev. **120**, 1758 (1960).

[16] Oak Ridge Technical Enterprises Corporation, Oak Ridge, Tennessee.

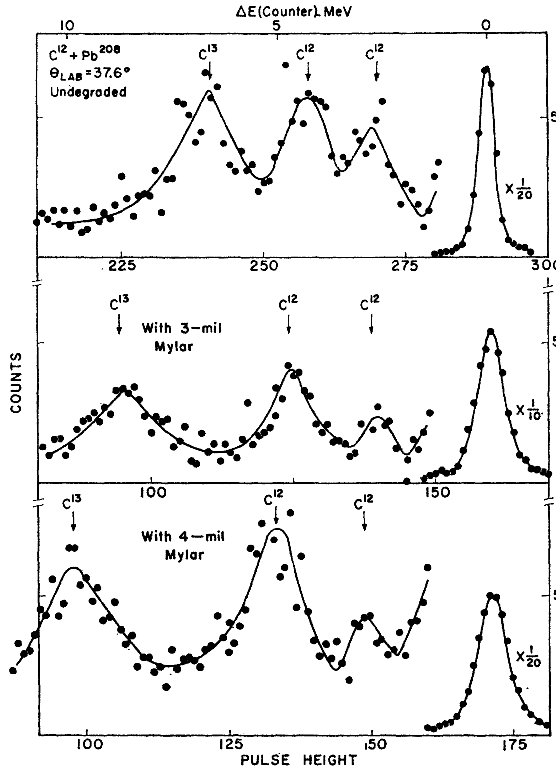


FIG. 2. Energy spectra of particles in $^{12}C+^{208}Pb$ for various thicknesses of the degrading foil. Note the amount of shift for the fourth peak as compared with that for the second and third peaks. The arrows from right to left are for $(^{12}C+^{208}Pb)^*$ ($Q=-2.7$ MeV), $(^{12}C+^{208}Pb)^*$ ($Q=-4.5$ MeV), and $(^{13}C+^{207}Pb)^*$ ($Q=-4.2$ MeV), respectively.

that they are $^{12}C$ peaks. However, the fourth peak corresponds to an excitation of 9 MeV (with 3-mil Mylar). On the other hand, if one assumes that the particles in the fourth peak are $^{13}C$ resulting from the $^{208}Pb(^{12}C,^{13}C)^{207}Pb$ reaction with an excitation energy of 4.2 MeV in the final nuclei, the positions of such a peak for absorbers of various thicknesses are indicated by the arrows. It is seen that the fourth peak follows closely the predicted positions for the $^{13}C$ particles. Consequently this peak can be identified as resulting from the $(^{12}C,^{13}C)$ transfer reaction. The mean position of the second peak from the right (from all available spectra) gives an excitation energy of 2.7±0.3 MeV, that of the third peak, 4.5±0.3 MeV, while the mean position of the transfer peak gives 4.2±0.5 MeV; the last figure includes the uncertainty arising from the absorber thickness.

The intensity of a peak should be independent of the absorber thickness. A change of intensity would be an indication of a mixture of different particles, some of them moving out from under the peak due to the difference in energy loss in the absorber. A change in intensity would also be affected by the change in the intensity of the tail of the elastic-scattering peak which extends underneath the peak.

In this connection, it should be noted that the intensity of the second peak from the right is lower with an absorber than without it. This reduction in the peak size is probably due to the presence of other particles resulting from one or more of the reactions: $^{208}Pb(^{12}C,^{13}C)^{207}Pb$, $^{208}Pb(^{12}C,^{14}N)^{206}Tl$, and $^{208}Pb(^{12}C,^{15}O)^{205}Hg$ where the mass differences render $Q$ values of $-2.4$, $-2.5$, and $-2.5$ MeV, respectively. Such contributions do not seem to exceed 30% of the total intensity. Aside from this possible 30% contribution to the peak in the top curve, the 2.7-MeV peak may be identified with the excitation of $^{208}Pb$ to its well-known 2.6-MeV state (see Fig. 3).

The 4.5-MeV peak may be due either to the excitation of $^{12}C$ to the 4.4-MeV state or to the excitation of $^{208}Pb$ to the 4.3-MeV state or to some of both (Fig. 3). Other states in $^{12}C$ or $^{208}Pb$ are not involved since the next level in $^{12}C$ is at 7.7. MeV while the nearest collective level in $^{208}Pb$ is at 3.2 MeV. Excitation of these levels would not contribute to the 4.5-MeV peak.

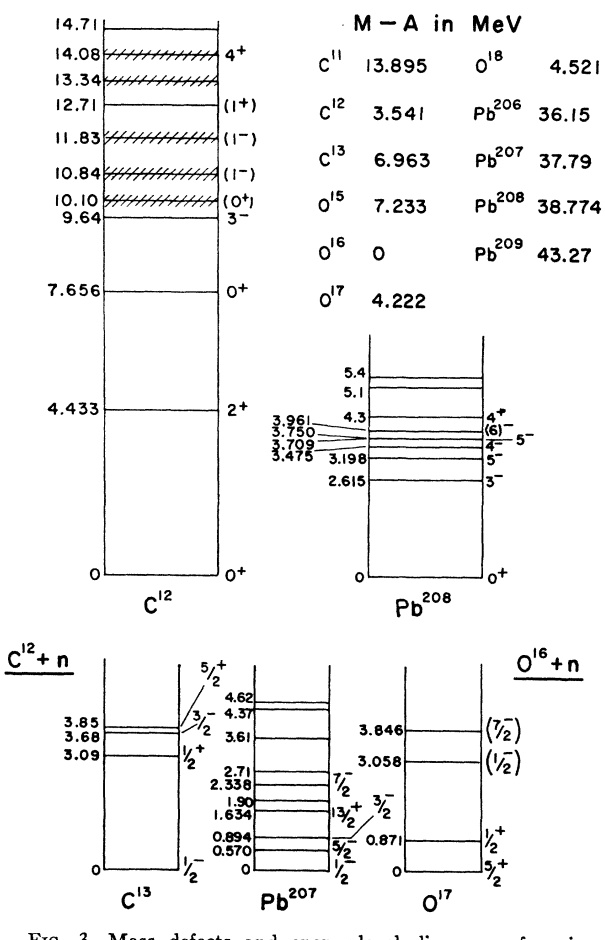


FIG. 3. Mass defects and energy-level diagrams of various nuclei involved in these experiments. The former are computed using atomic mass values given in the Trilinear Chart of Nuclides by W. H. Sullivan (U. S. Atomic Energy Commission, 1957). The latter are taken from F. Ajzenberg-Selove and T. Lauritsen, Nucl. Phys. 11, 1 (1959).

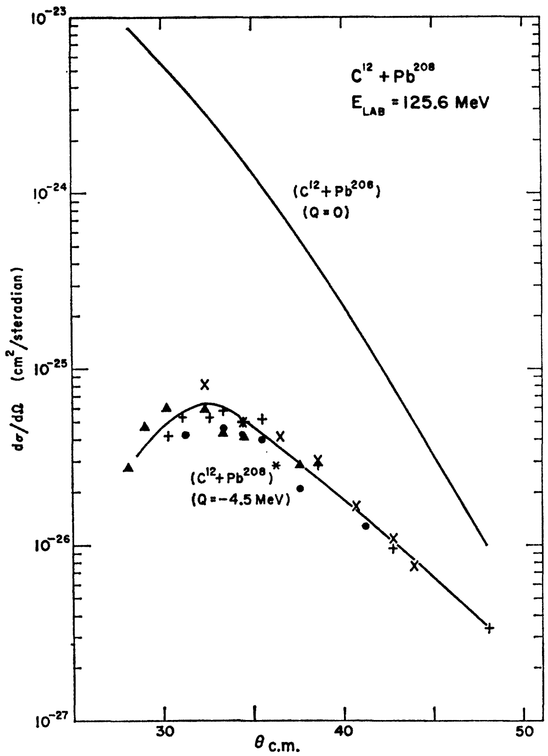


FIG. 4. Angular distribution in the center-of-mass system of the inelastic scattering leading to a state at 4.5 MeV. The distribution of the elastic scattering is also shown for comparison. ●, △, ×, and + indicate data taken with 0, 3, 1, and 3-mil Mylar degrading foils. The former two sets of data were taken in March 1963, the latter two in November 1962.

In the transfer reaction ($^{12}C$,$^{13}C$), the division of the excitation energy cannot be uniquely determined since there are several possible combinations of excitation of the final nuclei (see Fig. 3). Experimentally only the total excitation energy is measured.

The angular distributions for both inelastic scattering and the ($^{12}C$,$^{13}C$) neutron pickup reaction are shown in Figs. 4 and 5, together with the elastic-scattering distribution. The latter distribution agrees with an independent measurement by Baker.[17] The cross sections are accurate to +25%, −5% for the 2.7-MeV peak and +15%, −5% for the other peaks. The uncertainties arise mainly from the background subtraction.

It is seen that there is not much structure in the angular distributions. It should be noted that the detector subtends a scattering angle of about 2% which is equal to the expected period of oscillation that might appear from the diffraction of the projectile wave around the target nucleus. The poor angular resolution could have made the oscillations undetectable. However a careful investigation of the elastic scattering with good angular resolution[17] has failed to reveal any oscillations. The lack of oscillations in the angular distributions of the inelastic scattering is presumably real since the elastic and inelastic scattering are expected to be similar in this respect.[18] Furthermore, in the inelastic scattering of $^{14}N$ from $^{12}C$ at 28 MeV ($\eta=5$),[19] the oscillation in the angular distribution is almost non-existent while considerable oscillation appears in the elastic scattering. It has also been reported[20] that the inelastic scattering of 40-MeV alpha particles from $^{208}Pb$ ($\eta=9$) leading to the 2.6-MeV state showed a monotonic increase in the cross section with decreasing angle.

The inelastic cross sections in Figs. 4 and 5 are seen to level off at about 35°. The data at smaller angles are difficult to obtain due to the intense elastic scattering peak. Since the 4.5-MeV peak is further away from the elastic peak, data at somewhat smaller angles can be obtained. They show that there is a further decrease in the cross section at smaller angles.

When the angular distribution is transformed into a radial distribution[21] by assuming a Rutherford scatter-

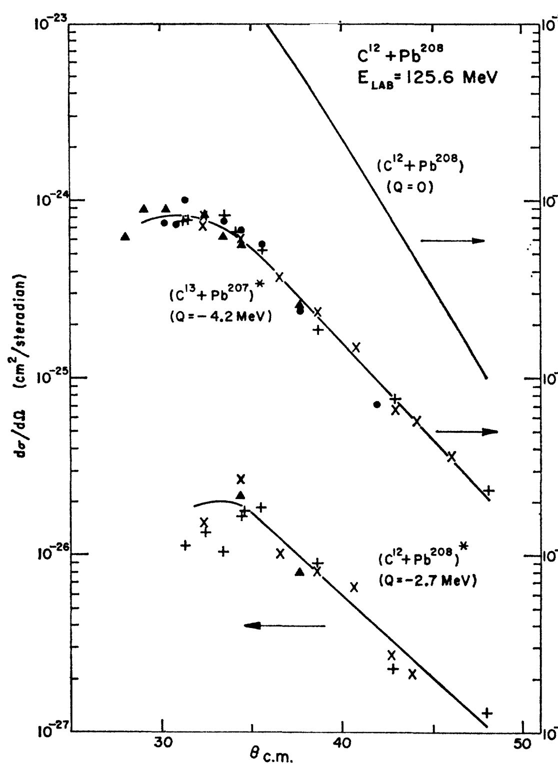


FIG. 5. Angular distributions in the center-of-mass system for the inelastic scattering leading to the 2.7-MeV state and for $^{208}Pb(^{12}C,^{13}C)^{207}Pb$. See caption to Fig. 4 for various symbols. Note that two ordinate scales are used.

[17] S. D. Baker, Ph.D. thesis, Yale University, 1963 (to be published).

[18] E. Rost and N. Austern, Phys. Rev. **120**, 1375 (1960).
[19] M. L. Halbert and A. Zucker, Phys. Rev. **121**, 236 (1961).
[20] G. W. Farwell, D. D. Kerlee, M. Rickey, and P. Robinson, Physics **22**, 1127 (1956).
[21] J. A. McIntyre, T. L. Watts, and F. C. Jobes, Phys. Rev. **119**, 1331 (1960).

ing trajectory for the projectile, the differential ross section $d\sigma/d\Omega$ is related to $d\sigma/dR_{\min}$ by the relation

$$\frac{d\sigma}{dR_{\min}}=\frac{-16E}{ZZ'e^2}\sin^3\left(\frac{\theta}{2}\right)\frac{d\sigma}{d\Omega},$$

where $E$ and $\theta$ are the energy and angle in the center-of-mass system, and $R_{\min}$ is the distance of closest approach of the projectile to the target nucleus. The maximum in the radial distribution occurs at $R_{\min}=13.3\times10^{-13}$ cm. This yields a value of $r_0=1.62\times10^{-13}$ cm, where $r_0$ is defined by $R_{\min}=r_0(A_1^{1/3}+A_2^{1/3})$, $A_1$ and $A_2$ being the atomic weights of $^{12}C$ and $^{208}Pb$. This value of $r_0$ is in agreement with those found in neutron transfer experiments.[22] The result indicates that the maximum cross section occurs at an angle corresponding to a grazing collision. One can understand the decrease in the cross section at large angles as the result of absorption when the trajectory of the particle passes the absorption radius of the target nucleus. Again, at the smaller angles, the cross section is expected to decrease when particles do not come within the range of the nuclear forces. The angular distribution of the transfer reaction also exhibits a monotonic increase with decreasing angle, typical of single-neutron-transfer reactions.[21]

### B. $^{16}O+^{208}Pb$

In the $^{12}C+^{208}Pb$ experiment, it was not possible to determine which nucleus was being excited to a state at about 4.5 MeV. Since the first excited state in $^{16}O$ is at 6.1 MeV, no uncertainty should arise at 4.5 MeV if $^{16}O$ nuclei are used as projectiles.

It is seen in the upper spectrum of Fig. 6 that there is one "inelastic scattering" peak. With absorbers, however, the shift of the peak position disagrees with that expected for $^{16}O$. The arrows indicate expected positions of the possible transfer products $^{17}O$ and $^{18}O$. In each case, both final nuclei are assumed to be in the ground state. The peak is seen to follow the calculated position for $^{17}O$ and not $^{18}O$; therefore the peak is identified as resulting from the $^{208}Pb(^{16}O,^{17}O)^{207}Pb$ reaction. The $Q$ value derived from the mean position of this peak determines the excitation energy of the final state of the system to be $(-0.2\pm0.5)$ MeV. The $^{17}O$ nucleus must, therefore, be in its ground state (see Fig. 3).

Since the peak obscures the two inelastic scattering peaks under investigation under normal circumstances, a very thick absorber was used to move the peak beyond the expected position of the 4.5-MeV peak (see bottom spectrum in Fig. 6). There is no sign of a 4.5-MeV peak. Inspection of Fig. 6 shows also that the 2.6-MeV inelastic-scattering peak is small. Earlier[23] the peak did not show clearly, so further data have been taken. With somewhat better resolution than in the earlier publication, there now does appear to be an inelastic scattering peak at 2.6 MeV. The cross section obtained from the spectrum shows that the inelastic scattering with $^{16}O$ is smaller than with $^{12}C$ by a factor of $(2\pm0.5)$.

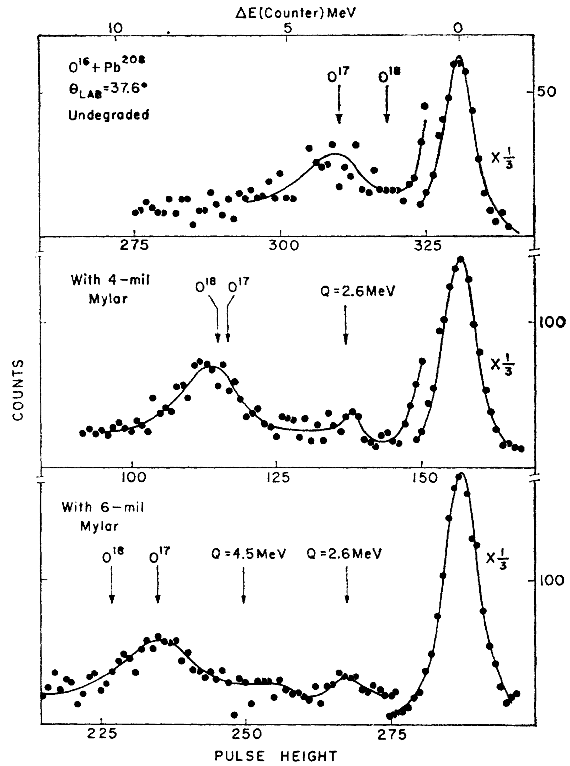


FIG. 6. Energy spectra of particles in $^{16}O+^{208}Pb$. Note that the second peak follows the $^{17}O$ arrow more closely than the $^{18}O$ arrow as the absorber thickness is varied.

The angular distribution for the transfer reaction has been measured and is shown in Fig. 7 along with the elastic scattering distribution; the latter again agreed well with earlier results.[17] The differential cross section for the $(^{16}O,^{17}O)$ reaction is approximately equal to that for $^{208}Pb(^{12}C,^{13}C)^{207}Pb$ reaction.

## IV. DISCUSSION OF RESULTS

The significance of the various peaks in the energy spectra (Figs. 2 and 6) will now be considered. The elastic scattering peak will not be discussed here, however, since investigation of the elastic scattering has recently been made by Baker[17]; in addition, an earlier study has also been made by Kerlee, Reynolds, and Goldberg.[24]

Comments on the angular distributions of the inelastically scattered projectiles have already been made

[22] A. Zucker, Ann. Rev. Nucl. Sci. **10**, 27 (1960).

[23] K. H. Wang and J. A. McIntyre, *Proceedings of the Third Conference on Reactions between Complex Nuclei*, edited by A. Ghiorso, R. M. Diamond, and H. E. Conzett (University of California Press, Berkeley, 1963), p. 31.

[24] D. D. Kerlee, H. L. Reynolds, and E. Goldberg, Phys. Rev. **127**, 1224 (1962).

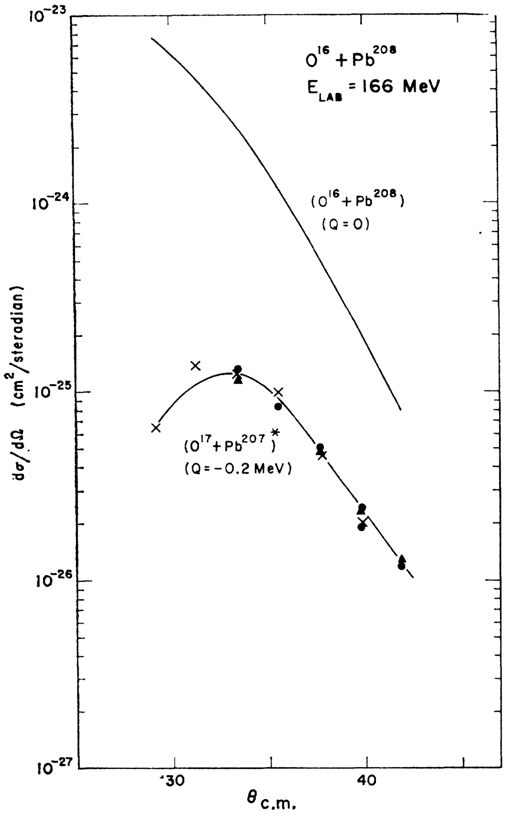


FIG. 7. Angular distribution in the center-of-mass system of $^{17}O$ from the $^{208}Pb(^{16}O,^{17}O)^{207}Pb$ reaction together with the elastic scattering distribution for comparison. ●, △, and ✕ indicate data taken with 0-, 4-, and 6-mil Mylar degrading foils.

in the last section. It was shown there that the distributions can be understood in terms of semiclassical trajectories for the projectiles and that a radius of interaction between the projectile and the target nucleus is determined.

### A. The 2.7-MeV Peak

This peak appears for both the $^{12}C$ and the $^{16}O$ inelastic scattering and undoubtedly corresponds to the excitation of the 2.6-MeV level in $^{208}Pb$. The cross section for the excitation of the $^{208}Pb$ by the $^{12}C$ nucleus is $2\pm0.5$ times as large as for excitation by the $^{16}O$ nucleus at the same angle. This result is difficult to understand in terms of semiclassical factors which should dominate the interactions studied here ($\eta\sim25\gg1$). In semiclassical terms, the Rutherford trajectories followed by the projectiles depend only on the velocity of the projectiles.[25] Since the $^{12}C$ and $^{16}O$ projectiles have the same velocities in the experiments under discussion, they should follow the same trajectories. That this analysis is a valid one is shown by the close similarity between the elastic-scattering cross sections for $^{12}C$ and $^{16}O$ in Figs. 4 and 7. In particular, at the angle where the $^{16}O$ excitation of $^{208}Pb$ was studied ($\theta_{\text{c.m.}}=40.2°$—see Fig. 7) the scattering cross sections for $^{12}C$ and $^{16}O$ differ by less than 20%. Thus, from a semiclassical point of view, the inelastic-scattering process should also be very similar for the two projectiles. The difference in the inelastic-scattering cross sections may then depend on the difference in the dynamical structure of the easily deformed $^{12}C$ and the more spherical $^{16}O$.

A distorted-wave Born approximation (DWBA) calculation would be required to determine whether the $^{12}C$ and $^{16}O$ inelastic-scattering experiments do yield the same distortion parameter $\beta_\lambda$ for the two interactions.[18] However, present DWBA computer programs are not extensive enough to calculate the interaction studied here where partial waves with $l>100$ must be considered. Thus, until an accurate calculation for the inelastic scattering can be made, the significance of the factor of 2 difference in the excitation of the 2.6-MeV level by $^{12}C$ and $^{16}O$ cannot be determined. Also, since $\beta_\lambda$ cannot be calculated at present from the data, it is impossible to compare the inelastic $^{12}C$ result with the $\beta_\lambda$ found for the 2.6-MeV excitation of $^{208}Pb$ using the inelastic-electron-scattering process.

### B. The 4.5-MeV Peak

The 4.5-MeV peak appears only for the $^{12}C$ scattering (Fig. 2). It occurs either because of the excitation of the 4.4-MeV level in $^{12}C$ or the 4.3-MeV level in $^{208}Pb$. Both levels could be excited *a posteriori*: the 4.4-MeV level in $^{12}C$ is known to be strongly excited by heavy projectiles[4] while the 4.3-MeV level in $^{208}Pb$ is a collective level that is excited by inelastic electron scattering.[3]

The determination of which excitation is more dominant may be inferred from the $^{16}O$ data (Fig. 6). Here, there is little, if any, 4.5-MeV excitation. This contrasts with that observed in the $^{12}C$ spectra where the 4.5-MeV peak is much larger than that at 2.7 MeV. The reduction in intensity of the 4.5-MeV excitation relative to that of 2.7 MeV suggests then that the 4.5-MeV peak corresponds to the excitation of the $^{12}C$ projectile rather than the $^{208}Pb$ nucleus.

### C. The Neutron-Transfer Reactions

The appearance of these reactions is surprising for at least two reasons:

(1) The cross sections for the reactions are large. With one exception,[11] they are twice as large as any previous transfer cross section measured in this energy range.[21] This is particularly striking when it is realized that the neutron transferred to the projectile is extracted from the double magic $^{208}Pb$ nucleus.

---

[25] The force between the projectiles is $ZZ'e^2/r$ while the mass of the projectile is $AM=2ZM$, where $M$ is the mass of the nucleon. Neglecting reduced-mass corrections, the acceleration of the projectile will be force/mass$=(ZZ'e^2/r)/2ZM=Z'e^2/2rM$, so that the acceleration is independent of the projectile. Thus, different projectiles having the same velocity will follow the same trajectories.

(2) In both the ($^{12}$C,$^{13}$C) case and the ($^{16}$O,$^{17}$O) case, the neutron transfer reaction leads predominantly to one level in the final nucleus. This result again contradicts the experience gained with neutron-transfer reactions. Except at the lowest energies,[26] the transfer of the neutron has been found to proceed to many excited states of the final nucleus.[27,21]

It is possible to understand these surprising effects to some degree, once the nature of the selected nuclear states in $^{13}$C and $^{17}$O have been determined. From the measurement of the $Q$ value of the reaction, it was determined that the $^{17}$O was in its ground state after the ($^{16}$O,$^{17}$O) reaction. The ground state of the $^{17}$O nucleus is known to be a single particle $d_{5/2}$ state.[28]

On the other hand, the assignment of the excitation in the ($^{12}$C,$^{13}$C) reaction is not unique. There are four states in $^{13}$C consistent with the $Q$ value determined in the experiment. Of the four, three, namely the 0-, 3.09-, and 3.85-MeV states are known to be single-particle states corresponding to a $p$, $s$, or $d$ neutron about the $^{12}$C core.[29] All of them have relatively large neutron widths in the $^{12}$C$(d,p)^{13}$C reaction; therefore, they would more likely be populated than the 3.68-MeV state in the present ($^{12}$C,$^{13}$C) reaction. These states have "analogs"[30] in $^{17}$O. In particular, Thomas[30] found that the interactions between an $s$ nucleon and a $^{12}$C or $^{16}$O core were characterized by a potential which was very similar in both cases. In the present experiment of ($^{16}$O,$^{17}$O), the reaction definitely leads to the $d_{5/2}$ ground state in $^{17}$O and there is little, if any, transfer to either the $p$ or $s$ state. It seems most reasonable then that the reaction ($^{12}$C,$^{13}$C) also leads to the $d_{5/2}$ single-particle state at 3.85 MeV in $^{13}$C.

It is interesting that other particle-transfer experiments have shown an enhanced amount of transfer involving the $d_{5/2}$ shell in this region of the periodic table. Harvey *et al.*[12] found, for $(\alpha,d)$ reactions on $^{12}$C and $^{16}$O targets, that both transferred nucleons were captured in $d_{5/2}$ shells about the $^{12}$C and $^{16}$O cores. Also, Kaufmann and Wolfgang[11] found that for the projectiles $^{12}$C, $^{14}$N, $^{16}$O, and $^{19}$F, the largest neutron transfer cross section occurred for the ($^{19}$F,$^{18}$F) reaction, again, a $d_{5/2}$ neutron is being transferred while for the other transfer reactions, $p$ neutrons are involved.

It is not clear just why the $d_{5/2}$ states are thus singled out. For the ($^{16}$O,$^{17}$O) reaction, of course, they are the lowest energy states, but this is not true for the ($^{12}$C,$^{13}$C) reaction. There is one known factor favoring the $d$-state against the $p$-state transfer and that is the conservation of angular momentum.[12,31] For the conditions of this experiment, the orbital angular momentum of each nucleon in the $^{12}$C and $^{16}$O nuclei about the center of the $^{208}$Pb nucleus is approximately $5\hbar$. Thus, the higher internal orbital angular momentum shells in the $^{13}$C and $^{17}$O nuclei will be favored for picking up the $p_{1/2}$ neutron from the $^{208}$Pb nucleus. It would be most interesting therefore to test this hypothesis by studying these reactions at lower energies where the angular conditions would be more fully satisfied.

In conclusion, then, it has been shown that for some, as yet not completely understood, reason the transfer of neutrons to the $d_{5/2}$ shell is enhanced. This enhanced transfer has already been found and studied by Harvey *et al.*[12] In addition, the enhancement can be made to account for the fact that these neutron-transfer cross sections are larger than any measured before with the exception of the ($^{19}$F,$^{18}$F) reaction.[11]


## ACKNOWLEDGMENTS

We take pleasure in expressing our appreciation to people who have helped with the experiments at various stages. Dr. S. D. Baker in particular helped in setting up the equipment as well as in collecting data. The scattering chamber was designed with the cooperation of A. Nicolaeff and constructed by C. J. Sneider. Discussions with Professor D. A. Bromley, Dr. J. C. Hiebert, and Dr. G. T. Garvey have also been most helpful. The cooperation of the accelerator crew under the direction of Professor E. R. Beringer and L. Baron is gratefully acknowledged.


[26] L. C. Becker and J. A. McIntyre, Phys. Rev. **138**, B339 (1965).
[27] See, e.g., M. L. Halbert and A. Zucker, Phys. Rev. **108**, 336 (1957); K. S. Toth, *ibid.* **121**, 1190 (1961) and **123**, 582 (1961).
[28] J. P. Elliott and A. M. Lane, *Handbuch der Physik*, edited by S. Flügge (Springer-Verlag, Berlin, 1957), Vol. 39, p. 241.
[29] W. E. Burcham, *Handbuch der Physik*, edited by S. Flügge (Springer-Verlag, Berlin, 1957), Vol. 40, p. 1.
[30] R. G. Thomas, Phys. Rev. **88**, 1109 (1952).
[31] G. Breit (private communication).